JOURNAL OF THERMOPHYSICS AND HEAT TRANSFER
Vol. 22, No. 4, October–December 2008

Finite Propagation of Heat Transfer in a Multilayer Tissue

Kuo-Chi Liu* and Po-Jen Cheng†
Far East University, Hsin-Shih, Tainan 744, Taiwan, Republic of China

DOI: 10.2514/1.37267

The concept of finite heat propagation velocity is applied to study the bioheat transfer problem in skin, which is stratified into epidermis, dermis, and subcutaneous layers. This paper proposes a modified numerical scheme and the analytical method to analyze the problem with the instantaneous surface heat flux. The numerical results are in a good agreement with the analytical solution that evidences the rationality and reliability of the present results. We discussed the deviations between the thermal wave model of bioheat transfer and the Pennes model. The predicted results depict that the time derivative of heat flux, the relaxation time, and the composite structure significantly affect the thermal propagation behavior. The effects of $\tau_1 \partial q(0,t)/\partial t \neq 0$ on the results from the equation for the thermal wave model of bioheat transfer are also distinct. The finite propagation effect should be described in the heating surface boundary condition.

Nomenclature

B, C, D, E	=	coefficients
c	=	specific heat of tissue, J/kg · °C
c_b	=	specific heat of blood, J/kg · °C
k	=	thermal conductivity, W/m · °C
L	=	length of tissue, m
ℓ	=	distance between two neighboring nodes, m
m	=	node number at the boundary surface
q_m	=	metabolic heat generation, J/m^3
q_r	=	heat source for spatial heating, J/m^3
q_w	=	amplitude of sinusoidal surface heating, J/m^3
s	=	Laplace transform parameter
T	=	temperature of tissue, °C
T_b	=	arterial temperature, °C
T_0	=	initial temperature of tissue, °C
t	=	time, s
$u(t)$	=	step function
V	=	heat propagation velocity in tissue, m/s
w_b	=	perfusion rate of blood, kg/m^3 · s
x	=	space coordinate, m
α	=	thermal diffusivity, m^2/s
θ	=	elevation temperature, $\theta = T - T_0$, °C
θ_0	=	initial elevation temperature, °C
$\bar{\theta}$	=	Laplace transform of θ
λ	=	parameter defined in Eq. (10)
ρ	=	density, kg/m^3
τ	=	relaxation time, s

Subscripts

i	=	node number
j	=	number of layer
k	=	number of subspace domain

I. Introduction

BECAUSE of medical treatment or accident, skin is probably exposed to a flash fire, laser irradiation, or contacted with hot substances. These situations would generate an instantaneous and high-rate heating on the surface of skin and might result in burn injuries. Investigations on such bioheat transfer behaviors are helpful to avoid thermal injuries and establish thermal protections. To predict the behavior of bioheat transfer in living tissues, the Pennes model is the most commonly used one among many bioheat transfer models [1] for simplicity and validity. The Pennes bioheat transfer equation describes the thermal behavior based on the classical Fourier's law and depicts an infinitely fast propagation of thermal signal. In reality, accumulating enough energy to transfer to the nearest element would take time in the process of heat transfer. In homogenous materials such as common metals, the accumulating time ranges (or relaxation time) from 10^{-8} to 10^{-14} s [2–4]. The heating processes are mostly much longer than this time scale, which is why the phenomenon of finite heat propagation is difficult to observe in common metals. However, the living tissues are highly nonhomogeneous, and the velocity of heat transfer in tissues should be limited. Since the concept of finite heat propagation velocity received the attention from relevant researchers [5–9], the paradox that occurred in the classical heat transfer model was solved.

The literature [2–4] reported the relaxation time in biological bodies to be 20–30 s. Mitra et al. [10] found the relaxation time for processed meat is on the order of 15 s and reconfirmed the order of magnitude of the values obtained by Kaminski [3]. The experimental investigation made by Roetzel et al. [11] showed the value of relaxation time to be about 2 s for processed meat. The preceding literature further support the phenomenon of finite thermal propagation velocity in the process of bioheat transfer. As a result, the thermal wave model of bioheat transfer [12,13] is introduced to investigate the physical mechanisms and behaviors of heat transfer in living tissues. The relationship between the heat flux vector and the thermal disturbance in the thermal wave model is described as [5–9]

$$\bar{q} + \tau \frac{\partial \bar{q}}{\partial t} = -k \nabla T \tag{1}$$

where τ is the relaxation time and can be approximated by $\tau = \alpha / V^2$. Conductivity, time, thermal diffusivity, and heat propagation velocity are denoted by k, t, α, and V, respectively. The time derivative term of heat flux in Eq. (1) mathematically described the effect of the relaxation time (or the finite propagation effect).

Some literatures have studied and analyzed the problems of bioheat transfer in skin. Most of their computational analysis is performed using the Pennes bioheat transfer equation. In accordance with the contents of the literature [5–9], the thermal wave behavior of heat transfer is obvious in the shorter heating processes. This paper attends to investigate the temperature distribution in skin with instantaneous surface heating for more understanding to the thermal wave propagation behavior of bioheat transfer. The fundamental solution of the thermal wave model of bioheat transfer is difficult to obtain. Various numerical methods [13–19] for solving the relevant

Received 23 February 2008; revision received 7 June 2008; accepted for publication 7 June 2008.

*Professor, 49 Chung Hua Road; kuochi.liu@msa.hinet.net or kcliu@cc.feu.edu.tw.
†Associate Professor, Department of Mechanical Engineering.

problems have been developed. A numerical method may encounter some mathematical difficulties for the non-Fourier heat conduction problem with the discontinuous time-dependent surface heat flux [16,17]. Because skin is regarded as a layered composite of epidermis, dermis, and subcutaneous [19], the complex boundary conditions raise the difficulty to solve the present problem. As a result, a modified numerical scheme based on the Laplace transform is developed to overcome such mathematical difficulties and analyze the present problem as well as the analytical method. The effects of the difference in the relaxation time for each layer and deviations between the thermal wave model of bioheat transfer and the Pennes model are investigated. The effects of the term $\tau\partial q/\partial t$ on the heating surface boundary condition or the temperature distributions are also explored and cleared up.

II. Mathematical Formulation

To consider the finite heat propagation effect, the thermal wave model of bioheat transfer (TWMBT) is proposed as

$$\nabla\cdot(k\nabla T)+w_b c_b(T_b-T)+q_m+q_r+\tau\left(-w_b c_b\frac{\partial T}{\partial t}+\frac{\partial q_m}{\partial t}+\frac{\partial q_r}{\partial t}\right)=\rho c\left(\frac{\tau\partial^2 T}{\partial t^2}+\frac{\partial T}{\partial t}\right) \tag{2}$$

Here, ρ, c, and T denote density, specific heat, and temperature of tissue, respectively. The specific heat is c_b, w_b is the perfusion rate of blood, q_m is the metabolic heat generation, and q_r is the heat source for spatial heating. T_b is the arterial temperature and regarded as a constant. Equation (2) is a hyperbolic equation and is more mathematically complex than the traditional Pennes bioheat equation. As $\tau=0$, Eq. (2) become the Pennes bioheat equation.

This paper focuses on studying the one-dimensional bioheat transfer problem in skin with the instantaneous surface heating. In reality, skin is stratified into epidermis, dermis, and subcutaneous layers, as shown in Fig. 1. The three layers have different physiological and thermal properties. Heat is assumed to be incident on the skin, and so the spatial heating is equal to zero. The 1-D form of Eq. (2) with constant thermal parameters for $q_m=$ constant and $q_r=0$ is written as

$$k\frac{\partial^2 T}{\partial x^2}+w_b c_b(T_b-T)+q_m-\tau w_b c_b\frac{\partial T}{\partial t}=\rho c\left(\frac{\tau\partial^2 T}{\partial t^2}+\frac{\partial T}{\partial t}\right) \tag{3}$$

Then, the initial steady temperature distribution $T_0(x,0)$ in skin can be derived from Eq. (3) as

$$k\frac{\partial^2 T_0}{\partial x^2}+w_b c_b(T_b-T_0)+q_m=0 \tag{4}$$

Subtracting Eq. (4) from Eq. (3) leads to

$$\rho c\tau\frac{\partial^2\theta}{\partial t^2}+(\rho c+\tau w_b c_b)\frac{\partial\theta}{\partial t}+w_b c_b\theta-k\frac{\partial^2\theta}{\partial x^2}=0 \tag{5}$$

where the elevation temperature θ is defined as $\theta=T-T_0$.

As skin is subjected to a flash fire, a short and high-rate heating is developed on the surface of skin. Heat losses from the surface can be neglected. Therefore, this study has the initial conditions

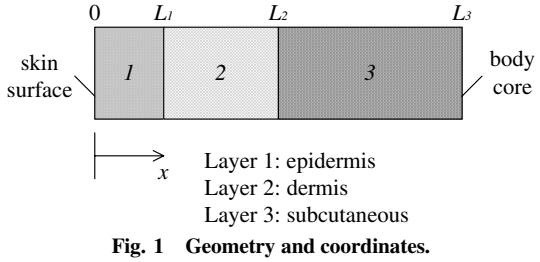

Fig. 1 Geometry and coordinates.

$$\theta(x,0)=0 \quad \text{and} \quad \frac{\partial\theta(x,0)}{\partial t}=0 \tag{6}$$

and the boundary conditions

$$k\left(\frac{\partial\theta}{\partial x}\right)=-\left(1+\tau\frac{\partial}{\partial t}\right)q=-\left(1+\tau\frac{\partial}{\partial t}\right)\{q_0[u(t)-u(t-t_h)]\} \quad \text{at } x=0 \quad \text{for } t>0 \tag{7}$$

and

$$\theta=0 \quad \text{at } x=L \quad \text{for } t>0 \tag{8}$$

where t_h is the heating duration, q_0 is the constant surface flux, and u is a step function.

For short duration of the instantaneous heating, the literature [13] ignored the finite propagation effect from the heating surface boundary condition. In other words, the boundary condition (7) can be written as

$$k\left(\frac{\partial\theta}{\partial x}\right)=-q=-q_0[u(t)-u(t-t_h)] \quad \text{for } t>0 \quad \text{and} \quad x=0 \tag{9}$$

For this point of view, further discussion is done in this study.

The boundary conditions at the interfaces of two adjacent layers are obtained from the assumption that temperature and heat flux are continuous.

III. Analysis

First, the Laplace transform method is employed to map the transient problem into a steady one. Equation (5) and the boundary conditions can be written in the transform domain for the initial conditions Eq. (6) as

$$\frac{\mathrm{d}^2\tilde{\theta}_j}{\mathrm{d}x^2}-\lambda_j^2\tilde{\theta}_j=0 \quad \text{for } j=1,2,3 \tag{10}$$

$$\frac{\mathrm{d}\tilde{\theta}_1}{\mathrm{d}x}=-\tilde{p}q_0(1-e^{-t_h s})\frac{1}{s} \quad \text{for } x=0 \tag{11a}$$

$$\tilde{\theta}_j=\tilde{\theta}_{j+1} \quad \text{for } x=L_j \quad \text{and} \quad j=1,2 \tag{11b}$$

$$\frac{k_j}{\tau_j s+1}\frac{\mathrm{d}\tilde{\theta}_j}{\mathrm{d}x}=\frac{k_{j+1}}{\tau_{j+1}s+1}\frac{\mathrm{d}\tilde{\theta}_{j+1}}{\mathrm{d}x} \quad \text{for } x=L_j \quad \text{and} \quad j=1,2 \tag{11c}$$

and

$$\tilde{\theta}=0 \quad \text{for } x=L_3 \tag{11d}$$

where

$$\lambda_j^2=\frac{1}{k_j}[\tau_j\rho_j c_j s^2+(\rho_j c_j+\tau_j w_b c_b)s+w_b c_b] \quad \text{for } j=1,2,3 \tag{12}$$

$$\tilde{P}=\frac{(\tau_1 s+1)}{k_1} \quad \text{for } \tau_1\partial q(0,t)/\partial t\neq 0 \tag{13a}$$

or

$$\tilde{p}=\frac{1}{k_1} \quad \text{for } \tau_1\partial q(0,t)/\partial t=0 \tag{13b}$$

where s is the Laplace transform parameter with respect to t. The function θ is written as $\tilde{\theta}$ in the Laplace domain. The subscript j denotes the layer number.

The interfacial boundary condition introduces the complexity and causes some mathematical difficulties for directly solving the present problem in the temperature domain. As a result, this paper develops a numerical scheme, and the analytical method based on the Laplace transform method is presented.

A. Numerical Analysis

The present paper divides the whole space domain into several subspace domains. For the continuity of the heat flux and temperature within layer j, the following conditions are required for the interior nodes in layer j:

$$\tilde{\theta}_{j,k}(x_i) = \tilde{\theta}_{j,k+1}(x_i) \quad \text{for } i = k, \qquad k = 2, \ldots, n-1 \tag{14}$$

and

$$\frac{\mathrm{d}\tilde{\theta}_{j,k}(x_i)}{\mathrm{d}x} = \frac{\mathrm{d}\tilde{\theta}_{j,k+1}(x_i)}{\mathrm{d}x} \quad \text{for } i = k, \qquad k = 2, \ldots, n-1 \tag{15}$$

where the subscripts i and k denote the node number and the subspace domain number, respectively.

The governing algebraic equations of the present problem can be derived from Eqs. (14) and (15). Before performing the derivation of the governing algebraic equations, $\tilde{\theta}$ should be approximated by using the nodal temperatures and shape functions within a small subspace domain. The shape functions should be carefully chosen for getting a more accurate result. Poor selection of the shape functions may produce severe numerical oscillations near the jump discontinuities and affect the accuracy and stability of the numerical results [20]. Owing to this reason, the present work derives the shape functions from the governing Eq. (10).

For the subspace domain k, $[x_i, x_{i+1}]$, the analytical solution of the governing Eq. (10) subjected to the boundary conditions

$$\tilde{\theta}_{j,k}(x_i) = \tilde{\theta}_{i,j} \quad \text{and} \quad \tilde{\theta}_{j,k}(x_{i+1}) = \tilde{\theta}_{i+1,j} \tag{16}$$

is easily obtained as

$$\tilde{\theta}_{j,k}(x) = \frac{1}{\sinh \lambda_j \ell_j}[\sinh \lambda_j (x_{i+1} - x)\tilde{\theta}_{i,j} + \sinh \lambda_j (x - x_i)\tilde{\theta}_{i+1,j}] \tag{17}$$

where ℓ_j denotes the length of the subspace domain or the distance between two neighboring nodes. Similarly, the analytical solution of Eq. (10) in the interval $[x_{i-1}, x_i]$, $\tilde{\theta}_{j,k-1}(x)$, can be obtained.

Substituting the shape functions $\tilde{\theta}_{j,k}(x)$ and $\tilde{\theta}_{j,k-1}(x)$ and Eq. (14) into Eq. (15) leads to the following discretized form for the interior nodes in layer j:

$$C_{i-1}\tilde{\theta}_{i-1,j} + C_i\tilde{\theta}_{i,j} + C_{i+1}\tilde{\theta}_{i+1,j} = 0 \tag{18}$$

where the coefficients C_{i-1}, C_i, and C_{i+1} are given as

$$C_{i-1} = C_{i+1} = 1.0 \tag{19a}$$

and

$$C_i = -2 \cosh \lambda_j \ell_j \tag{19b}$$

The discretized form for the node at the interface of layer j and layer $j+1$ can be obtained from the chosen shape functions and the boundary condition Eq. (11c) as

$$C_{i-1,j}\tilde{\theta}_{i-1,j} + C_{i,(j,j+1)}\tilde{\theta}_{i,(j,j+1)} + C_{i+1,j+1}\tilde{\theta}_{i+1,j+1} = 0 \quad \text{for } x = L_j \quad \text{and} \quad j = 1, 2 \tag{20}$$

where

$$C_{i-1,j} = \frac{k_j}{(\tau_j s + 1)} \frac{\lambda_j}{\sinh \lambda_j \ell_j} \tag{21a}$$

$$C_{i,(j,j+1)} = -\frac{k_j}{(\tau_j s + 1)} \frac{\lambda_j}{\sinh \lambda_j \ell_j} \cosh \lambda_j \ell_j - \frac{k_{j+1}}{(\tau_{j+1} s + 1)} \frac{\lambda_{j+1}}{\sinh \lambda_{j+1} \ell_{j+1}} \cosh \lambda_{j+1} \ell_{j+1} \tag{21b}$$

$$C_{i+1,j+1} = \frac{k_{j+1}}{(\tau_{j+1} s + 1)} \frac{\lambda_{j+1}}{\sinh \lambda_{j+1} \ell_{j+1}} \tag{21c}$$

Rearrangement of Eqs. (18) and (20) in conjunction with the discretized form of the boundary conditions yields the following matrix equation:

$$[C]\{\tilde{\theta}\} = \{F\} \tag{22}$$

where $[C]$ is a matrix with the complex number s, $\{\tilde{\theta}\}$ is a column vector representing the unknown nodal evaluation temperatures in the Laplace transform domain, and $\{F\}$ is a column vector representing the forcing term. The Gaussian elimination algorithm and the numerical inversion of the Laplace transform [21] are applied to compute the nodal temperatures in the physical domain.

B. Analytical Solution

The analytical solution of Eq. (10) can be written as

$$\tilde{\theta}_j = D_j e^{\lambda_j x} + E_j e^{-\lambda_j x} \quad \text{for layer } j, \qquad j = 1, 2, 3 \tag{23}$$

The coefficients in Eq. (23) are able to be obtained with the boundary conditions (11a–11d) and are described as

$$D_1 = E_1 - \frac{\tilde{p}}{\lambda_1}\tilde{q} \tag{24a}$$

$$E_1 = h_1 D_2 + h_2 E_2 \tag{24b}$$

$$D_2 = h_5 E_2 + h_6 \tag{24c}$$

$$E_2 = h_7 / h_8 \tag{24d}$$

$$D_3 = -E_3 e^{-2\lambda_3 L_3} \tag{24e}$$

$$E_3 = h_3 D_2 + h_4 E_2 \tag{24f}$$

where

$$h_1 = \frac{1}{2}\left(1 - \frac{\tau_1 s + 1}{\lambda_1 k_1} \cdot \frac{\lambda_2 k_2}{\tau_2 s + 1}\right) e^{(\lambda_1 + \lambda_2)L_1} \tag{25a}$$

$$h_2 = \frac{1}{2}\left(1 + \frac{\tau_1 s + 1}{\lambda_1 k_1} \cdot \frac{\lambda_2 k_2}{\tau_2 s + 1}\right) e^{(\lambda_1 - \lambda_2)L_1} \tag{25b}$$

$$h_3 = \frac{1}{2}\left(1 - \frac{\tau_3 s + 1}{\lambda_3 k_3} \cdot \frac{\lambda_2 k_2}{\tau_2 s + 1}\right) e^{(\lambda_3 + \lambda_2)L_2} \tag{25c}$$

$$h_4 = \frac{1}{2}\left(1 + \frac{\tau_3 s + 1}{\lambda_3 k_3} \cdot \frac{\lambda_2 k_2}{\tau_2 s + 1}\right) e^{(\lambda_3 - \lambda_2)L_2} \tag{25d}$$

$$h_5 = \frac{e^{-\lambda_2 L_1} - (e^{-\lambda_1 L_1} + e^{\lambda_1 L_1})h_2}{(e^{-\lambda_1 L_1} + e^{\lambda_1 L_1})h_1 - e^{\lambda_2 L_1}} \tag{25e}$$

$$h_6 = \frac{e^{\lambda_1 L_1}}{(e^{-\lambda_1 L_1} + e^{\lambda_1 L_1})h_1 - e^{\lambda_2 L_1}} \cdot \frac{\tilde{p}}{\lambda_1} \cdot \tilde{q} \tag{25f}$$

$$h_7 = [e^{-2\lambda_3(L_3 - L_2)} - 1]h_3 h_6 + e^{(\lambda_2 + \lambda_3)L_2} h_6 \tag{25g}$$

$$h_8 = [1 - e^{-2\lambda_3(L_3 - L_2)}](h_3 h_5 + h_4) - e^{(\lambda_3 - \lambda_2)L_2} - e^{(\lambda_3 + \lambda_2)L_2} h_5 \tag{25h}$$

and

$$\tilde{q} = -q_0(1 - e^{-t_h s})\frac{1}{s} \tag{26}$$

The preceding Eqs. (24a–24f) and (25a–25h) provide a complicated structure of the analytical solution for the triple-layer tissue. The composite interfaces of dissimilar materials raise the difficulty for solving such problems. The numerical inversion of the Laplace transform [21] is applied to perform the inverse transforms of Eq. (23) for θ. The analytical solution can be used to determine the accuracy of the present numerical results.

IV. Results and Discussion

Table 1 shows the values of relevant parameters used to perform all present computations in the present paper. At the same time, the skin surface temperature, the body core temperature, the relaxation time, the intensity of surface heat flux, and the heating duration are also specified as $T_s = 32.5\,^{\circ}\mathrm{C}$, $T_e = 37\,^{\circ}\mathrm{C}$, $\tau_1 = \tau_2 = \tau_3 = 20$ s, $q_0 = 83.2\ \mathrm{kW/m^2}$, and $t_h = 3$ s, respectively. Some parameter values were adjusted possibly for comparison and discussion, and are noted in each figure. Figures 2–8 show the computation results obtained by the present numerical method and the analytical method.

The value of temperature in skin is the sum of the initial temperature T_0 and the evaluation temperature θ. For the case in which the skin surface temperature T_s and the body core temperature T_e are assumed to be constant, the initial temperature distribution can be obtained from Eq. (4) with the follow boundary conditions:

$$T_{0,1}(0) = T_s \tag{27a}$$

$$T_{0,j}(L_j) = T_{0,j+1}(L_j) \quad \text{for } j = 1, 2 \tag{27b}$$

$$k_j \frac{\mathrm{d}T_{0,j}(L_j)}{\mathrm{d}x} = k_{j+1} \frac{\mathrm{d}T_{0,j+1}(L_j)}{\mathrm{d}x} \quad \text{for } j = 1, 2 \tag{27c}$$

and

$$T_{0,3}(L_3) = T_e \tag{27d}$$

Table 1 Values of relevant parameters for calculations [1]

	Blood	Epidermis	Dermis	Subcutaneous
c,J/kg · °C	3770	3600	3400	3060
w_b, kg/m^3 · s	——	0.0	1.5	1.25
k, W/m · °C	——	0.26	0.52	0.21
L, m	——	80×10^{-6}	0.002	0.01
ρ kg/m^3	1060	1200	1200	1000

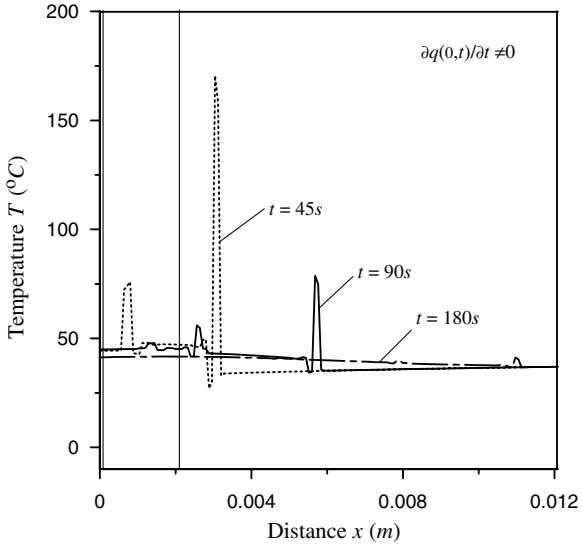

Fig. 2 Temperature distributions in skin with the effect of $\tau_1 \partial q(0,t)/\partial t \neq 0$ for various times.

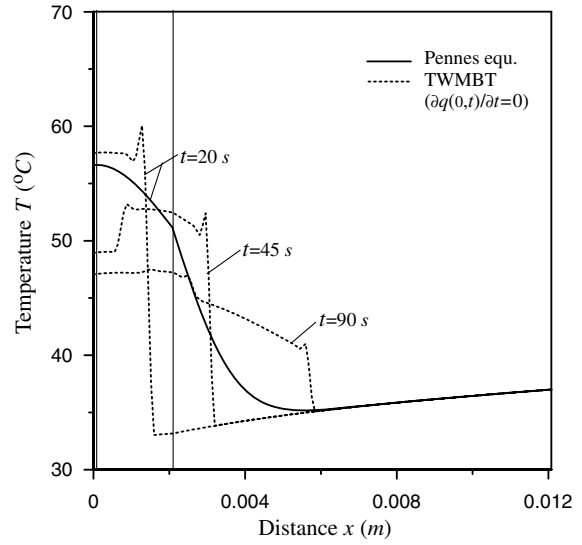

Fig. 3 Comparison between the results from TWMBT equation with $\partial q(0,t)/\partial t = 0$ and from the Pennes equation.

Thus, the initial temperature distribution in skin can be described mathematically as

$$T_{0,1} = -\frac{q_m}{2k_1}x^2 + A_1 x + B_1 \quad \text{for } 0 < x < L_1 \tag{28a}$$

$$T_{0,j} = A_j \cosh \beta_j x + B_j \sinh \beta_j x + \frac{S_j}{\beta_j^2} \quad \text{for } L_{j-1} \le x < L_j \quad \text{and} \quad j = 2, 3 \tag{28b}$$

where the coefficients are defined as

$$\beta_j = \sqrt{w_b c_b / k_j} \tag{29a}$$

$$S_j = (q_m + w_b c_b T_b)/k_j \tag{29b}$$

$$A_1 = \left[\frac{T_e - (S_3/\beta_3^2) - (H_3H_7 + H_1H_8)\cosh\beta_3L_3 - (H_3H_5 + H_1H_6)\sinh\beta_3L_3}{(H_4H_7 + H_2H_8)\cosh\beta_3L_3 + (H_4H_5 + H_2H_6)\sinh\beta_3L_3}\right] \tag{30a}$$

$$B_1 = T_s \tag{30b}$$

$$A_2 = H_3 + H_4A_1 \tag{30c}$$

$$B_2 = H_1 + H_2A_1 \tag{30d}$$

$$A_3 = H_7A_2 + H_8B_2 \tag{30e}$$

$$B_3 = H_5A_2 + H_6B_2 \tag{30f}$$

And then,

$$H_1 = -\frac{q_mL_1}{\beta_2L_2}\cosh\beta_2L_1 + \left(\frac{S_2}{\beta_2^2} + \frac{q_m}{2K_1}L_1^2 - T_s\right)\sinh\beta_2L_1 \tag{31a}$$

$$H_2 = \frac{k_1}{\beta_2k_2}\cosh\beta_2L_1 - L_1\sinh\beta_2L_1 \tag{31b}$$

$$H_3 = \frac{q_mL_1}{\beta_2L_2}\sinh\beta_2L_1 - \left(\frac{S_2}{\beta_2^2} + \frac{q_m}{2k_1}L_1^2 - T_s\right)\cosh\beta_2L_1 \tag{31c}$$

$$H_4 = -\frac{k_1}{\beta_2k_2}\sinh\beta_2L_1 + L_1\cosh\beta_2L_1 \tag{31d}$$

$$H_5 = \frac{k_2\beta_2}{k_3\beta_3}\sinh\beta_2L_2\cosh\beta_3L_2 - \cosh\beta_2L_2\sinh\beta_3L_2 \tag{31e}$$

$$H_6 = \frac{k_2\beta_2}{k_3\beta_3}\cosh\beta_2L_2\cosh\beta_3L_2 - \sinh\beta_2L_2\sinh\beta_3L_2 \tag{31f}$$

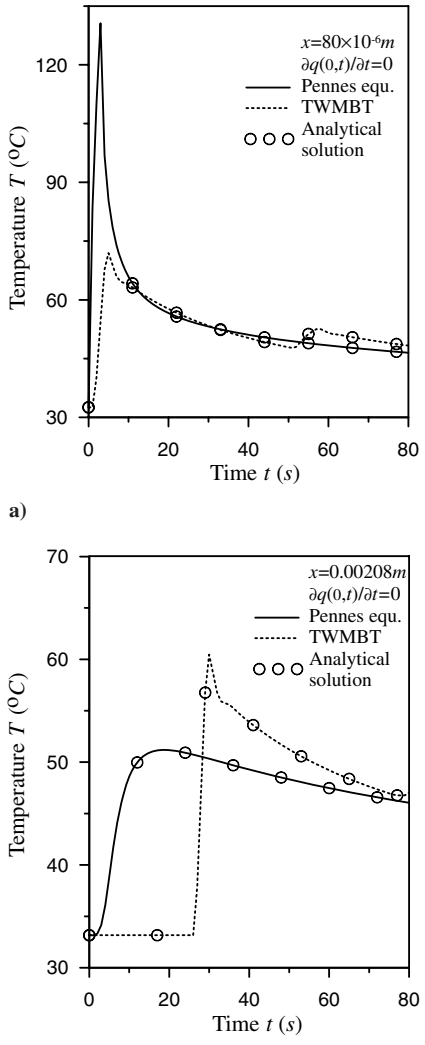

Fig. 4 Histories of temperatures with $\partial q(0,t)/\partial t = 0$ at a) $x = 80 \times 10^{-6}$ m and b) $x = 0.00208$ m.

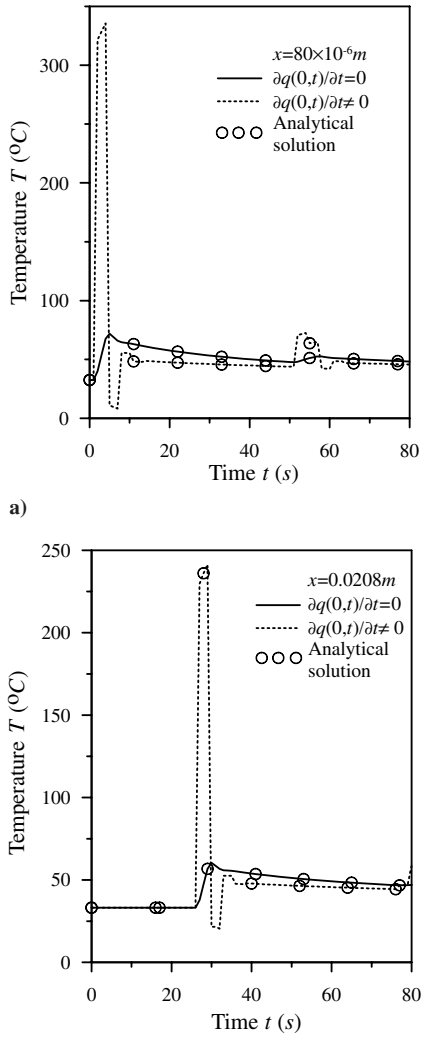

Fig. 5 Comparison of the transient temperatures with and without the effect of $\tau_1\partial q(0,t)/\partial t$ at a) $x = 80 \times 10^{-6}$ m and b) $x = 0.00208$ m.

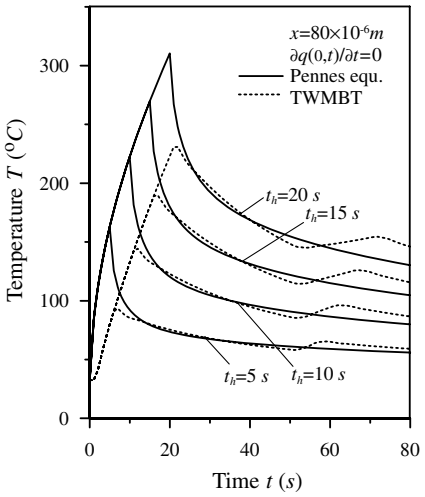

Fig. 6 Predictions of temperature at $x = 80 \times 10^{-6}$ m for various heating periods.

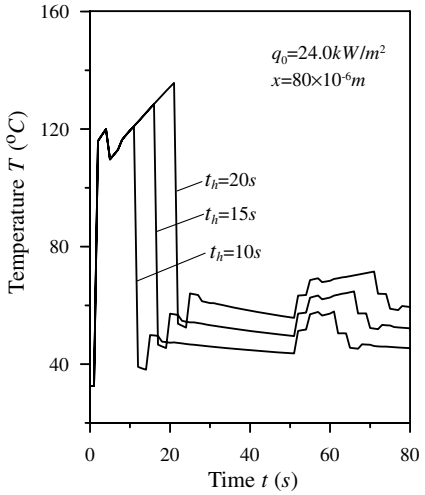

Fig. 7 Transient temperatures at $x = 80 \times 10^{-6}$ m for $\tau_1 \partial q(0,t)/\partial t \neq 0$ and $q_0 = 24.0$ kW/m^2.

$$H_7 = \cosh \beta_2 L_2 \cosh \beta_3 L_2 - \frac{k_2 \beta_2}{k_3 \beta_3} \sinh \beta_2 L_2 \sinh \beta_3 L_2 \qquad (31g)$$

$$H_8 = \sinh \beta_2 L_2 \cosh \beta_3 L_2 - \frac{k_2 \beta_2}{k_3 \beta_3} \cosh \beta_2 L_2 \sinh \beta_3 L_2 \qquad (31h)$$

As the literature [16,17] describes, the phenomenon of reflection and transmission would happen at the interface of two adjacent layers for the difference of thermophysical properties in the process of thermal wave propagation. The transmission–reflection behavior affects the temperature distribution and the temperature gradient in layered media. Figure 2 depicts the temperature distributions in skin with the effect of $\tau_1 \partial q(0,t)/\partial t \neq 0$ for various times. The initial thermal pulse has passed through the interfaces at $x = 80 \times 10^{-6}$ m and $x = 0.00208$ m for $t \geq 45$ s. The behavior of reflection and transmission at both of these interfaces forms multithermal pulses in skin at $t = 45$ and 90 s. The literature [16,17,22] states that the heat transfer ability of each layer is dominated by its thermophysical properties. When the thermal pulse propagates into the layer that has the better heat transfer ability, the reflected pulse will become downward. Because of thinness and thermophysical properties of

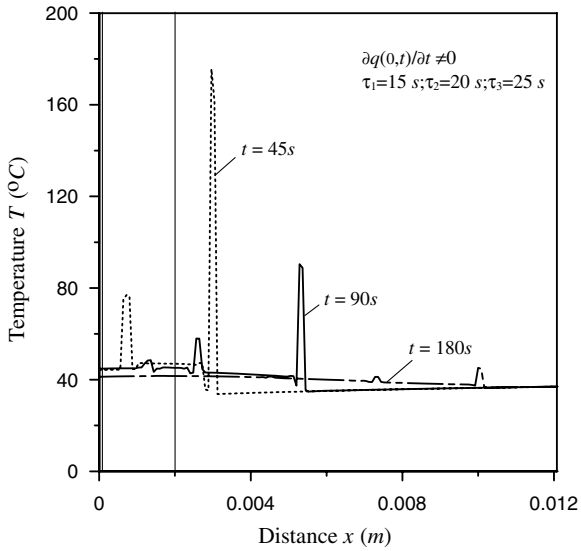

Fig. 8 Temperature distributions at various times for $\tau_1 \partial q(0,t)/\partial t \neq 0$, $\tau_1 = 15$ s, $\tau_2 = 20$ s, and $\tau_3 = 25$ s.

layer 1, a downward pulse follows the transmitted pulse, as shown in Fig. 2. As $t = 180$ s, the thermal pulses almost disappear for energy diffusion. On the other hand, the major difficulty in the numerical solution of the hyperbolic heat transfer problem is numerical oscillations near the sharp discontinuities [20]. The situation of multi-wave-fronts and the composite interfaces of dissimilar materials increase the difficulty for solving such problems. It can be seen that the present numerical results do not exhibit severe numerical oscillations in the vicinity of the jump discontinuity. Obviously, the present numerical scheme can successfully be applied to suppress these oscillations.

Further, to know the effect of $\tau_1 \partial q(0,t)/\partial t$ on the temperature distribution, the comparison between the results from the TWMBT equation with $\partial q(0,t)/\partial t = 0$ and those from the Pennes equation is presented in Fig. 3. It is observed from the comparison between Fig. 2 and Fig. 3 for $t = 45$ and 90 s that the effect of $\tau_1 \partial q(0,t)/\partial t$ on the temperature distribution cannot be ignored. It is worthy to reconsider whether the neglect to $\tau_1 \partial q(0,t)/\partial t$ is proper or not. As $\tau_1 = \tau_2 = \tau_3 = 20$ s, the propagation velocity of heat transfer in inner skin is still finite for $\tau_1 \partial q(0,t)/\partial t = 0$. Thus, Fig. 3 depicts the thermal wave fronts and the phenomenon of reflection and transmission for the results based on the thermal wave model of bioheat transfer. However, the initial heating pulse structure has been changed for $\partial q(0,t)/\partial t = 0$. The thermal pulses are not so steep and clearly visible, and the peak values are reduced, but the connection between the reflected and transmitted pulses is enhanced. The temperature distribution based on the Pennes equation shows the characteristics of the classical heat conduction law. Heat is transferred away from the skin surface sooner. There is a smooth temperature distribution in each layer.

Figures 4a and 4b depict histories of temperatures with $\partial q(0,t)/\partial t = 0$ at $x = 80 \times 10^{-6}$ m and $x = 0.00208$ m, respectively. The thermal wave model considers heat propagation in a medium at a finite speed. The thermal signal caused by the surface heating propagates to the locations $x = 80 \times 10^{-6}$ m and $x = 0.00208$ m, and needs a time period. The present results have this time period as $\Delta t = x/\sqrt{\alpha/\tau}$. It matches the definition of finite propagation velocity for the hyperbolic diffusion. The locations $x = 80 \times 10^{-6}$ m and $x = 0.00208$ m are at the initial status until the thermal signal reaches them. After that, the temperature jump is created. Because of the reflection–transmission effect at the interface $x = 0.00208$ m, the transient temperature of $x = 80 \times 10^{-6}$ m has an up-and-down variation around $t = 55$ s. Following the concept of finite propagation velocity, the elevated temperature from the Pennes equation quickly decreases, whereas a time lag exists for the disappearance of heat flow from the TWMBT equation. This

phenomenon is also observed in Fig. 4. Another finding, in which the numerical results coincide with the analytical solution, shows the accuracy of the present numerical results. However, the computation results in the literature [13] presented make a difference with the present results.

Figure 5 presents the comparison of the transient temperatures for $\tau_1 \partial q(0,t)/\partial t \neq 0$ with those for $\tau_1 \partial q(0,t)/\partial t = 0$ at $x = 80 \times 10^{-6}$ m and $x = 0.00208$ m. During $0 \text{ s} < t < 80$ s, the heat energy carried off by the perfusion blood is small. The cooling function of the blood perfusion does not affect the structure of the thermal wave yet. The influence of blood perfusion rate on the temperature distribution is insignificant during short times. The literature [23] states that if the thermal wave is caused by the pulsed surface heat flux, it has two wave fronts. This phenomenon is found in the result for $\tau_1 \partial q(0,t)/\partial t \neq 0$, but not for $\tau_1 \partial q(0,t)/\partial t = 0$. Evidently, the effect of $\tau_1 \partial q(0,t)/\partial t = 0$ changes the structure of the heating pulse and destroys the sharp thermal wave fronts. The thermal impact on the heating surface and the reflection–transmission phenomenon at the interfaces is weakened. As $\tau_1 \partial q(0,t)/\partial t \neq 0$, the thermal waves induce a higher temperature at the interfaces. The transient temperatures occasionally exhibit the behavior of oscillation for the reflection–transmission effect.

The thermal response in skin is concerned with the duration of heating. Figure 6 shows the predictions of temperature at the interface between epidermis and dermis, $x = 80 \times 10^{-6}$ m, for various heating periods. It is believed that the longer the heating duration, the more heat flux into the skin. Thus, the temperature increases with the heating duration. At the early times, the temperatures from the Pennes equation are high for the infinite propagation speed of heat transfer. The transient temperatures at $x = 80 \times 10^{-6}$ m for $\tau_1 \partial q(0,t)/\partial t \neq 0$ and $q_0 = 24.0 \text{ kW/m}^2$ are presented in Fig. 7. For the effect of thermal inertial on the heating surface, there are many bends in the curves of temperature variation. The results presented in Figs. 6 and 7 are developed in magnitude in a certain regulation.

The relaxation time τ represents the characteristic time needed for accumulating the thermal energy to the nearest element in nonhomogeneous inner structures and its value is concerned with the kind of structure. The preceding computations are performed with the assumption of $\tau = 20$ s for epidermis, dermis, and subcutaneous layers. For getting more information about the behavior of thermal wave in tissues, this paper further performs the computation for the assumption of $\tau_1 = 15$ s, $\tau_2 = 20$ s, and $\tau_3 = 25$ s. The temperature distributions at various times for $\tau_1 \partial q(0,t)/\partial t \neq 0$ are presented in Fig. 8. The different values of τ make solving the problem more difficult and need more mathematical technologies [22]. The numerical results still do not exhibit severe numerical oscillations in the vicinity of the jump discontinuity.

V. Conclusions

The thermal wave model of bioheat transfer and the Pennes model are applied to investigate the thermal response in a triple-layer tissue with instantaneous surface heating. Deviations between both models and the effects of $\tau_1 \partial q(0,t)/\partial t \neq 0$ on the results from the TWMBT equation are presented. Because of the effects of the reflection–transmission phenomenon at the interfaces, the discontinuous time-dependent surface heat flux creates multidiscontinuities in the temperature distribution, and the difficulty of solving the problem is increased. A modified discretization scheme based on the Laplace transform is proposed in the present paper. The numerical results are in agreement with the analytical solution. In addition, the term $\tau \partial q/\partial t$ is characteristic of the thermal wave model. The thermal wave effect dominates the heat transfer process for an extremely high rate of change of heat flux. The removal of $\tau \partial q/\partial t$ from the heating surface boundary condition for instantaneous heating would significantly affect the results. It changes the structure of the heating pulse and destroys the sharp thermal wave fronts. The thermal impact on the heating surface and the reflection–transmission phenomenon at the interfaces is weakened. Thus, how to use the thermal wave model of bioheat transfer to predict burn injury is worthy of further discussion.

References

[1] Arkin, H., Xu, L. X., and Holmes, K. R., "Recent Developments in Modeling Heat Transfer in Blood Perfused Tissues," *IEEE Transactions on Bio-Medical Engineering*, Vol. 41, No. 2, 1994, pp. 97–107. doi:10.1109/10.284920

[2] Luikov, A. V., *Analytical Heat Diffusion Theory*, Academic Press, New York, 1968.

[3] Kaminski, W., "Hyperbolic Heat Conduction Equation for Material with a Nonhomogenous Inner Structure," *Journal of Heat Transfer*, Vol. 112, No. 3, 1990, pp. 555–560. doi:10.1115/1.2910422

[4] Braznikov, A. M., and Karpychev, V. A., and Luikova, A. V., "One Engineering Method of Calculating Heat Conduction Process," *Inzhenerno Fizicheskij Zhurnal*, Vol. 28, No. 4, 1975, pp. 677–680.

[5] Cattaneo, C., "Sulla Conduzione de Calore," *Atti del Seminario Matematico E Fisico dell'Univ. di Modena*, Vol. 3, 1948, pp. 3–21.

[6] Vernotte, P., "Les Paradoxes de la Theorie Continue de L'equation de la Chaleur," *Comptes Rendus Hebdomadaires des Seances de l'Academie des Sciences*, Vol. 246, 1958, pp. 3154–3155.

[7] Weymann, H. D., "Finite Speed of Propagation in Heat Conduction, Diffusion, and Viscous Shear Motion," *American Journal of Physics*, Vol. 35, No. 6, 1967, pp. 488–496. doi:10.1119/1.1974155

[8] Sobolev, S. L., "Transport Processes and Traveling Waves in Systems with Local Nonequilibrium," *Soviet Physics, Uspekhi*, Vol. 34, No. 3, 1991, pp. 217–229. doi:10.1070/PU1991v034n03ABEH002348

[9] Özisik, M. N., and Tzou, D. Y., "On the Wave Theory in Heat Conduction," *Journal of Heat Transfer*, Vol. 116, No. 3, 1994, pp. 526–535. doi:10.1115/1.2910903

[10] Mitra, K., Kumar, S., Vedavarz, A., and Moallemi, M. K., "Experimental Evidence of Hyperbolic Heat Conduction in Processed Meat," *Journal of Heat Transfer*, Vol. 117, No. 3, 1995, pp. 568–573. doi:10.1115/1.2822615

[11] Roetzel, W., Putra, N., and Das, S. K., "Experiment and Analysis for Non-Fourier Conduction in Materials with Non-Homogeneous Inner Structure," *International Journal of Thermal Sciences*, Vol. 42, No. 6, 2003, pp. 541–552. doi:10.1016/S1290-0729(03)00020-6

[12] Yang, W. H., "Thermal (Heat) Shock Biothermomechanical Viewpoint," *Journal of Biomedical Engineering*, Vol. 115, No. 4B, 1993, pp. 617–621.

[13] Liu, J., Chen, X., and Xu, L. X., "New Thermal Wave Aspects on Burn Evaluation of Skin Subjected to Instantaneous Heating," *IEEE Transactions on Bio-Medical Engineering*, Vol. 46, No. 4, 1999, pp. 420–428. doi:10.1109/10.752939

[14] Shih, T. C., Kou, H. S., Liauh, C. T., and Lin, W. L., "Impact of Thermal Wave Characteristics on Thermal Dose Distribution During Thermal Therapy: A Numerical Study," *Medical Physics*, Vol. 32, No. 9, 2005, pp. 3029–3036. doi:10.1118/1.2008507

[15] Yang, C. Y., "Estimation of the Period Thermal Conditions on the Non-Fourier Fin Problem," *International Journal of Heat and Mass Transfer*, Vol. 48, No. 17, 2005, pp. 3506–3515. doi:10.1016/j.ijheatmasstransfer.2005.03.018

[16] Liu, K. C., "Analysis of Dual-Phase-Lag Thermal Behavior in Layered Films with Temperature-Dependent Interface Thermal Resistance," *Journal of Physics D: Applied Physics*, Vol. 38, No. 19, 2005, pp. 3722–3732. doi:10.1088/0022-3727/38/19/022

[17] Liu, K. C., "Analysis of Thermal Behavior in Multi-Layer Metal Thin-Films Based on Hyperbolic Two-Step Mode," *International Journal of Heat and Mass Transfer*, Vol. 50, Nos. 7–8, 2007, pp. 1397–1407. doi:10.1016/j.ijheatmasstransfer.2006.09.018

[18] Sharma, K. R., "Damped Wave Conduction and Relaxation in Cylindrical and Spherical Coordinates," *Journal of Thermophysics and Heat Transfer*, Vol. 21, No. 4, 2007, pp. 688–693. doi:10.2514/1.28692

[19] Özen, Ş., Helhel, S., and Çerezci, O., "Heat Analysis of Biological Tissue Exposed to Microwave by Using Thermal Wave Model of

Bio-Heat Transfer," *Burns, Including Thermal Injury*, Vol. 34, No. 12008, pp. 45–49.
doi:10.1016/j.burns.2007.01.009

[20] Lin, J. Y., and Chen, H. T., "Numerical Solution of Hyperbolic Heat Conduction in Cylindrical and Spherical Systems," *Applied Mathematical Modelling*, Vol. 18, No. 7, 1994, pp. 384–390.
doi:10.1016/0307-904X(94)90224-0

[21] Honig, G., and Hirdes, U., "A Method for the Numerical Inversion of Laplace Transforms," *Journal of Computational and Applied Mathematics*, Vol. 10, No. 1, 1984, pp. 113–132.
doi:10.1016/0377-0427(84)90075-X

[22] Liu, K. C., and Cheng, P. J., "Numerical Analysis for Dual-Phase-Lag Heat Conduction in Layered Films," *Numerical Heat Transfer, Part A: Applications*, Vol. 49, No. 6, 2006, pp. 589–606.
doi:10.1080/10407780500436865

[23] Honner, M., "Heat Waves Simulation," *Computers & Mathematics with Applications*, Vol. 38, Nos. 9–10, 1999, pp. 233–243.
doi:10.1016/S0898-1221(99)00278-3